Demonstration of Primary and Secondary Muscle Fiber Architecture of the Bovine Tongue by Diffusion Tensor Magnetic Resonance Imaging

Van J. Wedeen,* Timothy G. Reese,* Vitaly J. Napadow,†, and Richard J. Gilbert†
*NMR Center and Department of Radiology, Massachusetts General Hospital and Harvard Medical School, Boston, Massachusetts; and †Department of Mechanical Engineering, Massachusetts Institute of Technology, Cambridge, Massachusetts USA

ABSTRACT The myoarchitecture of the tongue is comprised of a complex array of muscle fiber bundles, which form the structural basis for lingual deformations during speech and swallowing. We used magnetic resonance imaging of the water diffusion tensor to display the primary and secondary fiber architectural attributes of the excised bovine tongue. Fiber orientation mapping provides a subdivision of the tongue into its principal intrinsic and extrinsic muscular components. The anterior tongue consists of a central region of orthogonally oriented intrinsic fibers surrounded by an axially oriented muscular sheath. The posterior tongue consists principally of a central region of extrinsic fibers, originating at the inferior surface and projecting in a fan-like manner in the superior, lateral, and posterior directions, and lateral populations of extrinsic fibers directed posterior-inferior and posterior-superior. Analysis of cross-fiber anisotropy indicates a basic contrast of design between the extrinsic and the intrinsic fibers. Whereas the extrinsic muscles exhibit a uniaxial architecture typical of skeletal muscle, the intrinsic core muscles, comprised of the verticalis and the transversus muscles, show strong cross-fiber anisotropy. This pattern is consistent with the theory that the tongue's core functions as a muscular hydrostat in that conjoint contraction of the transverse and vertical fibers enable the tissue to expand at right angles to these fibers. These findings suggest that three-dimensional analysis of diffusion tensor magnetic resonance imaging provides a structural basis for understanding the micromechanics of the mammalian tongue.

INTRODUCTION

The tongue is a structurally complex muscular organ of unique functional versatility. It is comprised of a network of interwoven skeletal muscle fibers that, in concert, produce the variations of shape and position necessary for swallowing and speech. Accordingly, the three-dimensional analysis of glossal architecture is indispensable to an understanding of its function. However, such analyses are confronted by significant methodological problems when addressed with conventional microscopic imaging methods. These problems include, first, the difficulty of defining quantitatively fiber organization at each location in the tissue, and second, the difficulty of accurately assembling these local data into a coherent and complete three-dimensional atlas (McLean and Prothero, 1991).

Magnetic resonance imaging (MRI) of the water diffusion tensor has been shown in a variety of tissues to have the capacity to noninvasively map tissue fiber architecture (Moseley et al., 1991; Douek et al., 1991; Basser et al., 1994; Garrido et al., 1994; Wedeen et al., 1995). We demonstrated in our previous study that diffusion tensor MRI of the sheep tongue can resolve local fiber orientation (Gilbert et al., 1998). The present work extends these findings by demonstrating that three-dimensional analyses of diffusion tensor MRI data can be used effectively to map complete glossal myoarchitecture. The display of fiber direction revealed by the attributes of the local diffusion tensor provides an immediate division of the tongue into its primary constituent muscles and, by the analysis of cross-fiber anisotropy, reveals essential features of muscle design. Most strikingly, high cross-fiber anisotropies in the core of the tongue, which are spatially coherent and perpendicular to the tongue's axis, signify its specialized capacity to lengthen forcibly, and so to act in opposition to the ensheathing longitudinal muscles of the tongue.

METHODS

Specimens

Magnetic resonance imaging (MRI) was performed on 4 ex vivo cow tongues obtained from Blood Farms (West Groton, MA). The excision was performed by making an incision from the thyroid prominence to the angle of the mandible to expose the tongue, followed by en bloc resection. Whole tongue specimens were refrigerated and scanned within 24 h of harvest.

MRI

Diffusion tensor MRI was performed on fresh excised cow tongues. Whole tongue specimens were refrigerated and scanned within 24 h of harvest. For each specimen, data were acquired for contiguous slices perpendicular to the anterior-posterior axis of the tongue. Data were acquired at 1.5 Tesla (T) with a 20-cm receive-transmit head coil and a diffusion-sensitive stimulated-echo pulse sequence (Merboldt et al., 1991) using single-shot echo-planar spatial encoding with echo time (TE) = 54 ms, mixing time (TM) = 480 ms, repetition time (TR) = 800 ms, and spatial resolution of $3 \times 3 \times 6$ mm. Using 16 signal averages, acquisitions completed in 3 min per slice yielded SNR = 40:1 (glossal-to-background magnitude ratio) in the unattenuated images S_0, and SNR = 20:1 in the attenuated images S_k.

Received for publication 4 March 1999 and in final form 16 October 2000.
Address reprint requests to Van J. Wedeen, M.D., NMR Center, Department of Radiology, Massachusetts General Hospital-East, 149 13th Street, Charlestown, MA. Tel.: 617-726-5822; Fax: 617-726-2241; E-mail: van@nmr.mgh.harvard.edu.

0006-3495/01/02/1024/05 $2.00

Diffusion sensitization utilized gradient pulses of amplitude $\|\mathbf{g}\| = 10$ mT m^{-1} and duration $\delta = 12$ ms, corresponding to a net spatial modulation $\|\mathbf{k}\| = 2\pi\gamma_H\delta\|\mathbf{g}\| = 32$ radian mm^{-1} (where γ_H is the proton gyromagnetic ratio and $\mathbf{k}$ is a column vector). Using an interpulse delay $\Delta = 500$ ms, the diffusion sensitivity $\|b\|$ was

$$\|b\| = \int_\Delta \mathbf{k}^T\mathbf{k}\, dt \approx \|\mathbf{k}\|^2\Delta \approx 511 \text{ mm}^2 \text{ s}^{-1} \quad (1)$$

Spatial modulations $\mathbf{k}_i$, $i = 1, \ldots, 6$, were applied for orientations corresponding to non-opposed edge-centers of a cube: $\mathbf{k}_i\|\mathbf{k}_i\|^{-1} \in \{\{\pm 1, 1, 0\}, \{1, 0, \pm 1\}, \{0, \pm 1, 1\}\}2^{-1/2}$ and also for $\mathbf{k}_0 = \mathbf{O}$. The diffusion tensor was computed at every location by inversion of the linear equation for diffusion attenuation for the present stimulated-echo pulse sequence

$$\log(S_k/S_0) = -\int_\Delta \mathbf{k}^T\mathbf{D}\,\mathbf{k}\, dt \approx -\Delta\mathbf{k}^T\mathbf{D}\,\mathbf{k} \quad (2)$$

where S_k is the signal amplitude observed after spatial modulation $\mathbf{k}$ and $\mathbf{D}$ is the diffusion tensor, a symmetric tensor of order 2 (Merboldt et al., 1991; Basser et al., 1994; Reese et al., 1995). Eq. 1 refers to the true spatial modulation $\mathbf{k}$ which is the diffusion encoding plus any other phase modulations arising from the imaging pulse sequence (Basser et al., 1994). A set of attenuation images $\log(S_{ki}/S_0)$ determines $\mathbf{D}$ uniquely only if the sensitization matrices $b_i = \mathbf{k}_i\mathbf{k}_i^T$ span the six-dimensional space of symmetric tensors, as for the present six gradients. Algebraic solution for $\mathbf{D}$ amplifies noise to a degree related to the condition number ($\mathbf{b}$) of the matrix $\mathbf{b} = \{\mathbf{k}_i\mathbf{k}_i^T\}$, the ratio of highest to smallest eigenvalues of $(\mathbf{b}^T\mathbf{b})^{1/2}$, necessarily real and positive, where ($\mathbf{b}$) = 1 is ideal.

Diffusion tensor images were displayed by color-coded 3D graphics. To depict fiber orientation, the diffusion tensor at each location was represented by an octahedron whose 3 axes were determined by the diffusion eigensystem: axes' endpoints are $\{\pm\lambda_i\mathbf{v}_i\}$, $i = 1, 2, 3$, where λ_i and $\mathbf{v}_i$ are, respectively, the ith eigenvalues and eigenvectors of the diffusion tensor $\mathbf{D}$ (Garrido et al., 1994). With conventional ordering $\lambda_i \geq \lambda_j$ for $i \geq j$, the principal fiber orientation at each location was indicated by the leading eigenvector $\mathbf{v}_1$ (Basser et al., 1994; Gmitro et al., 1993; Hajnal et al., 1991; Moseley et al., 1991; Wu et al., 1993). Octahedra were, in addition, color-coded using the standard assignment of vector components to color channels: $\{|v_{1x}|, |v_{1y}|, |v_{1z}|\} \rightarrow$ {red, green, blue} (see Fig. 1 color sphere inset). To display the cross-fiber structure of glossal myoarchitecture, the diffusion tensor at each location was also graphically represented as a cylinder whose central axis is $\mathbf{v}_3$ and whose ends are parallel to the local $\mathbf{v}_1$–$\mathbf{v}_2$ plane.

RESULTS

Mapping of principal fiber orientations allows for the identification of the tongue's primary muscular components. In Fig. 1, diffusion octahedra are rendered and color-coded so

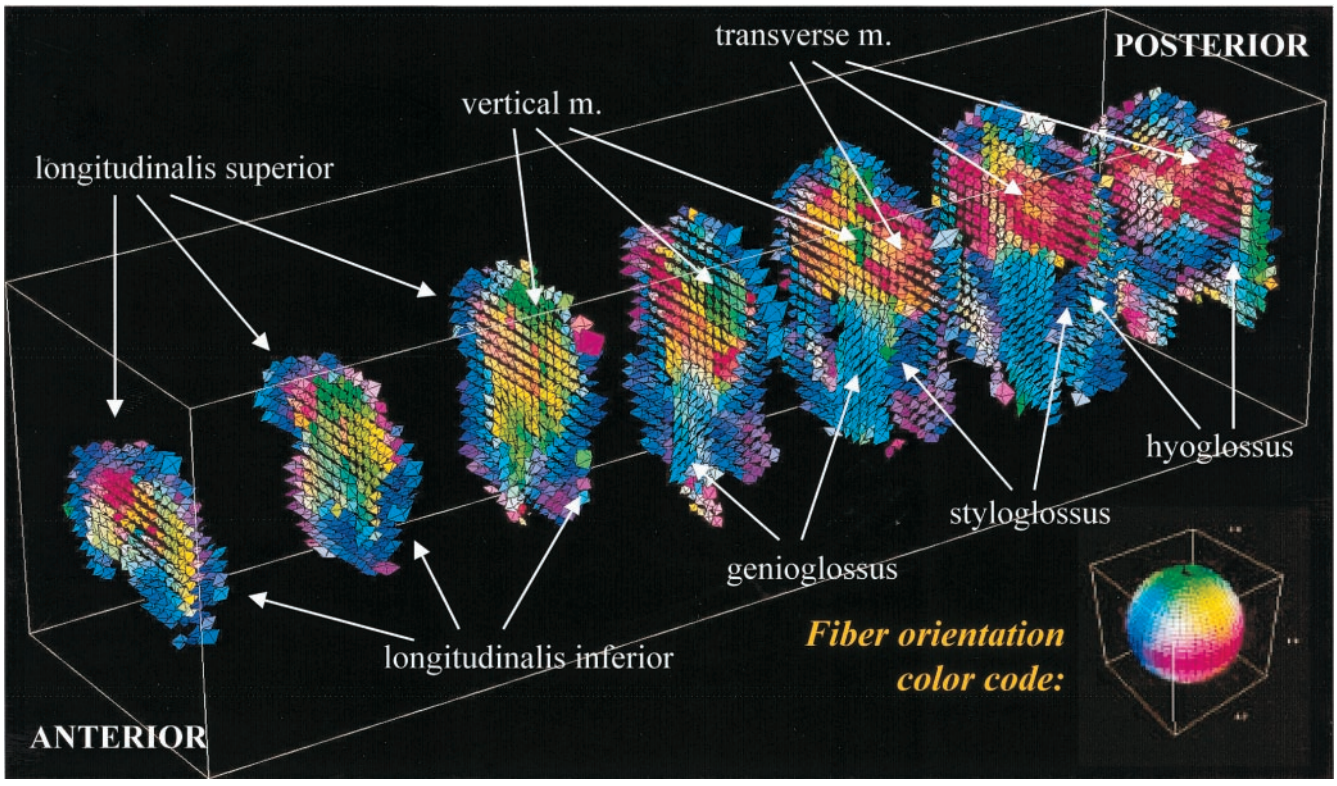

FIGURE 1 3D multislice diffusion tensor MRI of the bovine tongue. Coronal slices comprising the bovine tongue obtained by diffusion tensor imaging, with muscle components identified. At each voxel is placed an octahedron whose shape approximates the local diffusion tensor. The fiber orientation corresponds to the octahedron's long axis and its color to the 3D orientation. The color code is shown in the color sphere (*inset, lower right*). (*A*) Four coronal slices from the anterior tongue to the mid-tongue (tongue tip left to tongue center right). The contrast between the intrinsic tongue core and tongue sheath is conspicuous. The sheath consisting of superior and inferior longitudinal muscles is blue, corresponding to its longitudinal fiber orientation, and the tongue core is red and green, corresponding, respectively, to horizontal and vertical fiber orientations. (*B*) Four coronal slices from the mid-tongue to the posterior tongue (tongue center left to tongue posterior right). The extrinsic genioglossus and hyoglossus muscles are oblique; although both are coded blue-green, the octahedra show their distinct orientations: the genioglossus oriented antero-caudal and the hyoglossus oriented postero-caudal.

that the antero-posterior (A-P) fiber orientation is blue, left-right orientation is red, and superior-inferior orientation is green. Identified muscles include the superior and inferior longitudinal muscles (blue), the vertical muscle (green), the transverse muscle (red), and more posteriorly, the genioglossus and hyoglossus muscles, both blue-green, indicating obliquity in the sagittal plane. These muscles are organized in the anterior tongue as a core region of orthogonally oriented intrinsic fibers surrounded by a longitudinal sheath, and in the posterior tongue by a central region of extrinsic fibers projecting fan-like from the anterior-inferior surface, and lateral extrinsic fibers directed posterior-inferior and posterior-superior.

Two-dimensional lingual fiber organization is shown in Fig. 2, a rendering by cylinders of the data of Fig. 1, slice no. 3 from the anterior. This rendering shows a sharp contrast between the tongue's core, comprised of the vertical and transverse muscles, and its sheath of longitudinal muscles. At each location, the transaxial planes of the cylinder (its end-planes) indicates the plane in which local muscle fibers have highest angular dispersion (see Discussion). Within the tongue core, we see that these planes of maximum dispersion are approximately perpendicular to the A-P axis of the tongue, whereas in the sheath, these planes are concentric with the A-P axis and locally parallel to the nearby exterior surface. In the core of the tongue, these planes of fiber dispersion subtly tilt with respect to the A-P axis, forming bilateral whorls.

Regional changes of diffusion anisotropy provide further evidence of a core/sheath dichotomy. The diffusion anisotropy $A_{12} = \lambda_1 - \lambda_2 > 0$ is a scalar whose magnitude reflects the degree of fiber alignment. Fig. 3, a scatter-plot of A_{12} versus fiber azimuth angle relative to the A-P axis, shows that the distributions of principal orientation and anisotropy are correlated and bimodal. Specifically, voxels of the sheath, whose primary orientations are close to the A-P axis, have high A_{12}, indicating uniaxial fiber structure, whereas voxels of the core, whose orientations are most perpendicular to the A-P axis, have low A_{12}, consistent with multiaxial fiber structure.

DISCUSSION

We demonstrated in this study the ability of diffusion tensor MRI to resolve the constituent muscles of the tongue based on the principal direction of fibers and the angular dispersion of these fibers within the imaged element. In this

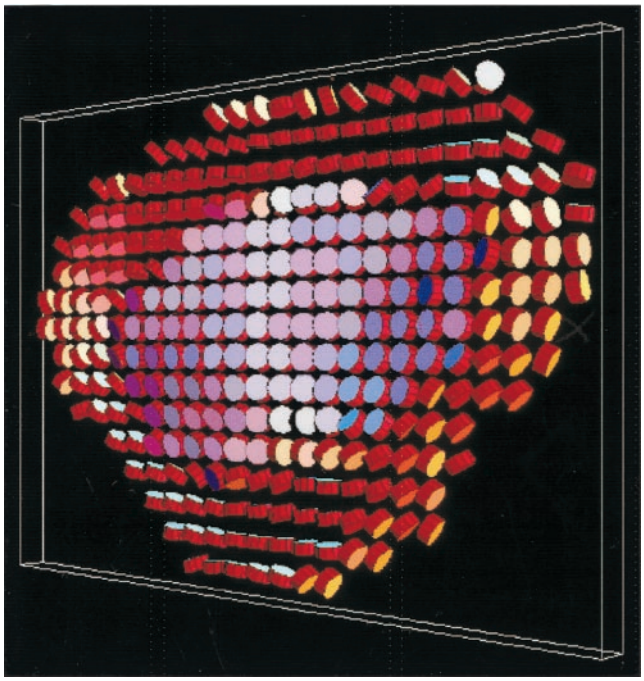

FIGURE 2 Geometric distribution of fiber angles in the anterior tip of the tongue (No. 3 of the slices in Fig. 1). At each voxel, the orientation of the first and second eigenvectors of the diffusion tensor is represented graphically by the end-planes of cylinders. At each location, end-planes of each cylinder indicate the plane in which local muscle fibers have maximal angular dispersion. Within the tongue core, we see that these planes of maximum dispersion are perpendicular to the A-P axis of the tongue, whereas in the sheath, these planes are concentric with the A-P axis and parallel to the nearby exterior surface. The colors displayed are arbitrary and used to enhance contrast between cylinder orientations.

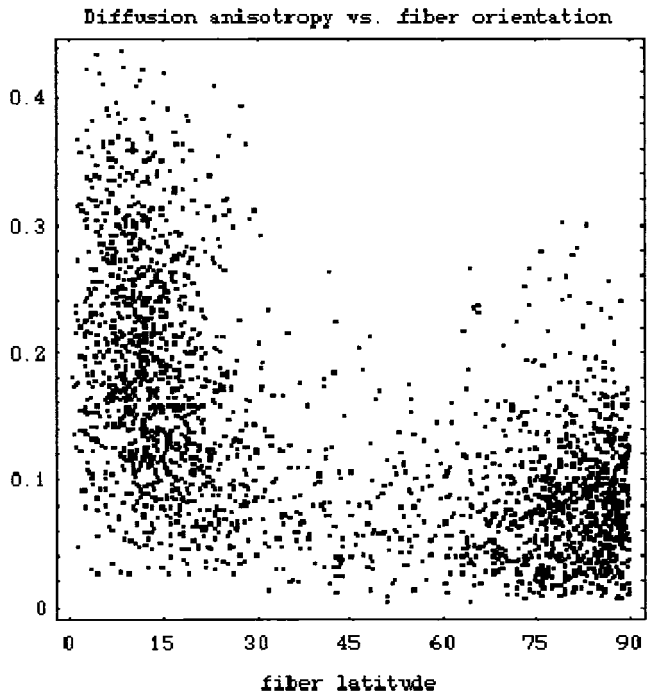

FIGURE 3 Diffusion anisotropy as a function of fiber azimuth angle. Diffusion fractional anisotropy $f = (\lambda_1 - \lambda_2)/\Sigma_i \lambda_i$ as a function of fiber azimuth angle with respect to the antero-posterior axis of the tongue. The tongue core, defined by fiber azimuth angle of 60° to 90° has a significantly lower anisotropy, $f = 0.09 \pm 0.01$ (mean, ± 95% confidence by *t*-test) than the sheath defined by 0° to 30° azimuth angle, where $f = 0.21 \pm 0.01$.

manner, we have created a complete three-dimensional anatomical atlas of the bovine tongue, thus providing a basis for studying the micromechanics of the tissue. In this formulation, the principal fiber orientation at each location in the image corresponds to the leading eigenvector of the diffusion tensor obtained by diffusion tensor imaging, whereas the second eigenvector identifies the orientation of maximum fiber angle dispersion in each voxel.

The organization of the intrinsic muscles of the tongue demonstrated in this study supports the hypothesis that lingual myoarchitecture enables this organ to function as a muscular hydrostat (Smith and Kier, 1989). In this model, simultaneous contractions of the vertical and horizontal core muscles cause the tongue (via conservation of volume) to protrude in the A-P axis at right angles to these fibers. The tongue core and sheath, therefore, comprise a functionally opposed pair, in which protrusion produced by bidirectional contraction of the core muscles is opposed by the retraction produced by unidirectional contraction of the longitudinal sheath muscles. From a physiological perspective, the horizontal and vertical deviations of the tongue tip that occur during deglutition and speech require simultaneous core protrusion and asymmetric sheath contraction. The functional distinction between the unidirectional contraction of the sheath and the bidirectional contraction of the core is reflected in the increased symmetry in the core between the first and second eigenvectors of the diffusion tensor (and is expressed by a reduction in the A_{12} anisotropy in the core region).

The structural and functional characteristics of the tongue core, similar to those of the myocardium, qualify it as a distinct type of muscle, a two-dimensional muscle that acts by expansion orthogonal to its fibers (LeGrice et al., 1995; Streeter, 1979; Wedeen et al., 1995; Tseng et al., 1997). The alternative view, that the transverse and longitudinal muscles of the core are functionally independent, may pose difficulty in an explanation of why these muscles interdigitate as finely as they appear to do. The question of the relative independence of muscle function in the tongue core may ultimately be resolved by experimental observation of lingual structure and function during the performance of specific actions (Napadow et al., 1998; Reese et al., 1997).

The evident axial symmetry of glossal fiber architecture deserves comment. Our data shows that the fibers of the tongue sheath, comprising the superior and inferior longitudinalis muscles, have maximum angular dispersion in planes that are oriented parallel to the nearby surface of the tongue and concentric with the A-P axis. This indicates that the muscle fibers of the sheath have a helical pitch relative to the axis of the tongue as they course antero-posteriorly. The tongue core also shows evidence of helical architecture, whereas the planar orientations of the core show subtle bilateral whorls. Helical fiber architecture is common in nature in the case of organs that must maintain strength during flexion. Examples include the longitudinal paravertebral muscles of fish, thought to enable high degrees of vertebral flexion without excessive stretching of the laterally situated fibers, the fibers of the cartilaginous skin of the shark, which form counter-rotating helices about the body axis to confer strength while resisting crimping when flexed, and the ventricular myocardium, whose fibers run helical about the ventricular axis from epicardium to endocardium, an arrangement believed to help equalize the force and extent of fiber shortening transmurally (Arts et al., 1984; 1994). Although the precise significance of helical fiber organization in the tongue sheath and fiber planes in the tongue core is uncertain, it is reasonable to postulate that this design exemplifies the ubiquitous logic of helical fiber architecture in combining flexibility with strength.

Our identification of three-dimensional muscle orientation requires the use of both color-coding and three-dimensional graphics, as most colors in this scheme do not correspond to unique three-dimensional orientations. This nonuniqueness results from the insensitivity of the code to the relative signs of vector components. For example, note that the genioglossus and hyoglossus muscles are both coded blue-green in Fig. 1, although they have distinct three-dimensional orientations. As one proceeds from posterior to anterior, the genioglossus descends inferiorly in the sagittal plane, while the hyoglossus rises superiorly. The nonuniqueness of this code could be addressed by using pair renderings whose color-codes are rotated three-dimensionally, so that a unique three-dimensional orientation would correspond to the pair of colors assigned at each point. This is, in effect, a six-color scheme, which is needed for the same reason that diffusion encoding requires at least six gradient directions, that is, that the space of homogeneous quadratic polynomials in 3D, $\Sigma_{1<i<j<3}\, x_i\, x_j$, is six-dimensional. It should be noted that these complex stratagems using graphics and multiple codes are necessary because human vision cannot detect six primary colors. Nevertheless, we believe that 3D graphics facilitates the visual appreciation of 3D geometry of these data. Furthermore, our experience suggests that the use of graphics like the present cylinders and octahedra (Garrido et al., 1994) that have sharp corners and edges facilitates the perception of tensor orientation in a superior fashion than the smooth ellipsoids that may be more faithful to the underlying mathematics (Basser et al., 1994).

We conclude that diffusion tensor MRI imaging of the tongue demonstrates primary structure, reflecting fiber orientations, and secondary structure, reflecting fiber angle dispersion. Orientational information of this nature efficiently divides the tongue into its principal muscular components. Further, patterns of anisotropy reveal more subtle and less familiar aspects of glossal fiber architecture. These findings suggest that the detailed geometric analysis of diffusion tensor MRI promise new insight into the functional anatomy of complex muscle systems.

REFERENCES

Arts, T., J. Meerbaum, R. S. Reneman, and E. Corday. 1984. Torsion of the left ventricle during the ejection phase in the intact dog. *Cardiovasc. Res.* 18:183–193.

Arts, T., F. W. Prinzen, L. H. Swoeckx, J. M. Riscken, and R. S. Reneman. 1994. Adaptation of cardiac structure by mechanical feedback in the environment of the cell: a model study. *Biophys. J.* 66:953–961.

Basser, P. J., J. Mattiello, and D. LeBihan. 1994. MR diffusion tensor spectroscopy and imaging. *Biophys. J.* 66:259–267.

Douek, P., R., Turner, J. Pekar, M. Patronas, and D. LeBihan. 1991. MR color mapping of myelin fiber orientation. *J. Comput. Assist. Tomogr.* 15:923–929.

Garrido, L., V. J. Wedeen, U. Spencer, and H. Kantor. 1994. Anisotropy of water diffusion in the myocardium of the rat. *Circ. Res.* 74:789–793.

Gilbert, R. J., T. G. Reese, S. J. Daftary, R. N. Smith, R. M. Weisskoff, and V. J. Wedeen. 1998. Determination of lingual myoarchitecture in whole tissue by NMR imaging of anisotropic water diffusion. *Am. J. Physiol.* 275:G363–G369.

Gmitro, A. F., and A. S. Alexander. 1993. Use of a projection reconstruction method to decrease motion sensitivity in diffusion weighed MRI. *Magn. Reson. Med.* 29:835–838.

Hajnal, J. V., M. Doran, A. S. Hall, A. G. Collins, A. Oatridge, J. M. Pennock, I. R. Young, and G. M. Bydder. 1991. MR imaging of anisotropically restricted diffusion of water in the nervous system: technical, anatomic, and pathologic considerations. *J. Comput. Assist. Tomogr.* 15:1–18.

LeCrice, I. J., Y. Takayama, and J. W. Covell. 1995. Transverse shear along myocardial cleavage planes provides a mechanism for normal systolic wall thickening. *Circ. Res.* 77:182–193.

McLean, M. and J. W. Prothero. 1991. Determination of relative fiber orientation in heart muscle: methodological problems. *Anat. Rec.* 232: 459–465.

Merboldt, K.-D., W. Hanicke, and J. Frahm. 1991. Diffusion imaging using stimulated echoes. *Magn. Reson. Med.* 19:233–235.

Moseley, M. E. J., J. Kucharczyk, H. S. Asgari, and D. Norman. 1991. Anisotropy in diffusion-weighted MRI. *Magn. Reson. Med.* 19:321–326.

Napadow, V. J., Q. Chen, V. J. Wedeen, and R. J. Gilbert. 1999. Intramural mechanics of the human tongue in association with physiological deformations. *J. Biomech.* 32:1–12.

Reese, T. G., R. M. Weisskoff, R. N. Smith, B. R. Rosen, R. E. Dinsmore, and V. J. Wedeen. 1995. Imaging myocardial fiber architecture in vivo with magnetic resonance. *Magn. Reson. Med.* 34:786–791.

Smith, K. K., and W. M. Kier. 1989. Trunks, tongues, and tentacles: moving with skeletons of muscle. *Am. Scientist.* 77:29–35.

Streeter, D. D. 1979. Gross morphology f fiber geometry of the heart. *In* Handbook of Physiology. B. M. Berne, N. Sperelakis, and S. R. Geigert, editors. Johns Hopkins Press, Baltimore. 61–112.

Tseng, W.-Y., T. G. Reese, R. E. Dinsmore, R. M. Weisskoff, and V. J. Wedeen. 1997. Progress in MRI myocardial structure and function using diffusion and strain. Proceedings of the 5th Annual Meeting of the International Society of Magnetic Resonance in Medicine, April 14–18, New York.

Wedeen, V. J., T. G. Reese, R. N. Smith, B. R. Rosen, R. M. Weisskoff, and R. E. Dinsmore. 1995. Mapping myocardial architecture with diffusion anisotropy MRI. Proceedings of the 3rd Annual Meeting of the International Society of Magnetic Resonance in Medicine, August 19–25, Cannes, France.

Wu, J. C., E. C. Wong, E. L. Arrindell, K. B. Simons, A. Jesmanowicz, and J. S. Hyde. 1993. In vivo determination of the anisotropic diffusion of water and the T1 and T2 times in the rabbit lens by high-resolution magnetic resonance imaging. *Invest. Ophthalmol. Vis. Sci.* 34: 2151–2158.